Hindawi
BioMed Research International
Volume 2023, Article ID 9981311, 15 pages
https://doi.org/10.1155/2023/9981311

Research Article

Optimization of Pregelatinized Taro Boloso-I Starch as a Direct Compression Tablet Excipient

Tamrat Balcha Balla,[1,2] **Nisha Mary Joseph**,[1] **and Anteneh Belete**[1,3]

[1]*Department of Pharmaceutics and Social Pharmacy, School of Pharmacy, College of Health Sciences, Addis Ababa University, P.O. Box 9086, Addis Ababa, Ethiopia*
[2]*School of Pharmacy, College of Health Sciences and Medicine, Wolaita Sodo University, P.O. Box 158, Wolaita Sodo, Ethiopia*
[3]*Center for Innovative Drug Development and Therapeutic Trials for Africa (CDT-Africa), College of Health Sciences, Addis Ababa University, Addis Ababa, Ethiopia*

Correspondence should be addressed to Tamrat Balcha Balla; tamrat.balcha@wsu.edu.et

Received 2 August 2022; Revised 5 January 2023; Accepted 7 January 2023; Published 16 January 2023

Academic Editor: Ahmed AH Abdellatif

Background. Tablets are still the most preferred means of drug delivery. The search for new and improved direct compression tablet excipients is an area of research focus. This is because the direct compression method overcomes the drawbacks of granulation methods of tablet production. It exempts several treatment steps associated with the granulation methods. The requirements for the powders to be directly compressible include flowability, low friction tendency, compressibility, and fast disintegration capacity. Taro Boloso-I is a new variety of *Colocasia esculenta* (L. Schott) yielding 67% more than a previously reported variety (Godare) in Ethiopia. This study is aimed at enhancing the flowability while keeping the compressibility and compactibility of the pregelatinized Taro Boloso-I starch. *Methods*. Central composite design was used for the optimization of two factors which were the temperature and duration of pregelatinization against 4 responses. The responses were angle of repose, Hausner's ratio, Heckel's yield pressure, and tablet breaking force. *Results and Discussions*. An increase in the temperature resulted in decrease in both the angle of repose and the Hausner ratio and that of time decreased angle of repose as well. The Heckel yield pressure was observed to increase with increasing levels of both temperature and time. The pregelatinized starch prepared by heating 15% slurry of Taro Boloso-I starch at the pregelatinization temperature of 66.22°C for 20 min showed desired flow property and compressibility. *Conclusions*. Pregelatinized Taro Boloso-I starch could be regarded as a potential direct compression excipient in terms of flowability, compressibility, and compactibility. The PGTBIS could perform better as filler and binder in direct compression tablets than the Starch 1500® in terms of compactibility.

1. Introduction

Solid dosage forms, especially tablets, are still the most preferred means of drug delivery [1, 2]. The search for new and improved direct compression tablet excipients is an area of research focus. This is because the direct compression method overcomes the drawbacks of granulation methods of tablet production. It exempts several treatment steps associated with the granulation methods. The requirements for the powders to be directly compressible include flowability, low friction tendency, compressibility, and fast disintegration capacity [3–7]. While starch is one of the leading polymers of preference for use as a pharmaceutical excipient, it has notable limitations including poor flowability and compressibility. However, native Taro Boloso-I starch is unique in that it has appreciable compressibility properties [8] while having very poor flow properties [9]. Unless some physical modifications such as pregelatinization or chemical modifications are employed to enhance the flow property, many of the potential functionalities such as direct compression properties of the native starch could not be utilized [10, 11]. Pregelatinization is claimed to improve the flowability of starches [12, 13]. It has been reported that the direct compression properties of starches would be enhanced following

changes in density, particle size and shape, and moisture content [14, 15] by pregelatinization better than acetylation [16]. The native Taro Boloso-I starch has low amylose to amylopectin ratio (20.7 ± 1.8 to 77.3 ± 2.1). Additionally, it has a high onset, peak, and endset temperatures of gelatinization, namely, 68.40°C, 75.46°C, and 84.40°C, respectively. It is comprised of polyhedral/angular granules existing in A-type polymorphism [9]. With the assumption that the process of pore reduction during compression of powders follows linear kinetics [17, 18], the Heckel model is the most accepted method for analyzing volume reduction with a pressure exerted on powders [19–21]. It involves plotting tablet densification versus the applied pressure. The linear portion of the graph has slope k and intercept A both of which are material constants. It represents the plastic deformation of the powder. This region is obtained by considering the line of best fit. Most of the time, the line of best fit is in the range of the compression pressure 50-150 MPa. The reciprocal of its slope (k) is equal to the Heckel yield pressure (P_y), the measure of the ability of the powder to deform plastically [19]. In the current study, the flow property and compressibility of pregelatinized Taro Boloso-I starch (PGTBIS) at different values of temperature and duration of pregelatinization were evaluated. The Heckel yield pressure (P_y) (using out-die-tablet Heckel model), angle of repose, compressibility index, and Hausner ratio were used as responses. The factors were optimized using the circumscribed central composite design (CCD) response surface methodology (RSM) [22–24].

2. Materials and Methods

2.1. Materials. Taro Boloso-I was obtained from Areka Agricultural Research Institute, located at Areka (300 km South of Addis Ababa), Wolaita, Ethiopia; sodium hydroxide (BDH Poole Co, UK) and sodium chloride (Sörensen, Lauren, Denmark) were used as obtained.

2.2. Preparation of Pregelatinized Starch. Taro Boloso-I starch (NTBIS) was extracted as per the methods described by Balla et al. [9] and pregelatinized using a method used by Odeku et al. [12]. Accordingly, a total of 13 aqueous slurries (15%, w/v) of NTBIS were heated in a water bath at specified temperatures (61.86–89.14°C) with continuous heating and uniform stirring for specified periods of time (11.72–68.28 min). The pregelatinized starches were then dried at 40 for 48 h and powdered in a laboratory grinder (Pulverisette 2, Fritsch, Germany) so that all the powders passed through a 224 μm aperture sieve. Finally, the samples were stored separately in tightly sealed glass containers.

2.3. Determination of Size Distribution, Density, Compressibility, and Flow Properties. The size distribution of PGTBIS particles was determined by using leather light diffractometer (Malvern Mastersizer 2000, Germany). For determination of bulk and tapped densities, the standard cylinder and tapped densitometer (ERWEKA, type SVM, Germany), respectively, were used. Bulk and tapped densities were used for the calculation of Carr's index and Hausner's ratio [25–26]. For the determination of true density (ρ_t), xylene displacement method was used with equation (1). Tablet true density (ρ_t) was computed as the weighted average of the component true densities. For the study of flow properties, the angle of repose and flow rate were determined by using the funnel method.

$$\rho = \frac{WS}{(X + W) - Y}, \tag{1}$$

where W, S, X, and Y stand for the weight of starch, the specific gravity of xylene (0.865), the weight of the flask filled with xylene, and the weight of flask with starch and xylene filled.

Heckel's plots: a single punch machine (Korsch AG XP1 K0010288, Germany) equipped with a round flat-faced stainless steel die cavity with a diameter of 10 cm was used for the preparation of the compacts. In advance of the compression, the punch faces and the die wall were lubricated with magnesium stearate suspension in 95% ethanol. Eight tablets of 300 ± 3 mg weight were prepared at each of 8 different compression pressures 38.22, 76.43, 114.65, 152.87, 191.08, 229.30, 267.52, and 305.58 MPa. Compact weight, tablet breaking force (TBF), diameter, and thickness of out-of-die tablets were measured 24 h after compression [22]. Compact density (tablet density, ρ_c) was calculated using its weight (w), diameter (d), and thickness (t). Out-of-die tablet relative density (D_{rel}) at any compression pressure was calculated as the ratio of compact density to true density and used for the calculation of the tablet porosity. The negative natural logarithm of tablet porosity was taken as its densification (equation (2)). Similarly, compression pressure was calculated from compression force in kN and tablet diameter (d). Finally, graph of $-\ln(1 - D_{rel})$ versus pressure (in MPa) was plotted to analyze compression properties of the powder compacts (equation (3)). The linear portion of the plot was obtained from the line of best fit using the Origin Software 7 (Origin LabTM Corporation, USA) such that the correlation coefficient was reasonably close to 1. Constant "A" (extrapolated intercept of the straight portion of the Heckel plot) was used to calculate the relative density just before deformation (D_A) (equation (4)). D_A per se, along with relative density at a point applied pressure equals zero (D_0), was used to calculate the phase of densification at low pressure, D_b (equation (5)) [22]. D_0 had been determined from the ratio of bulk density to true density.

$$\text{Densification} = -\ln(1 - D_{rel}), \tag{2}$$

$$-\ln(1 - D_{rel}) = \text{kP} + A, \tag{3}$$

$$D_A = 1 - e^{-A}, \tag{4}$$

$$D_b = D_A - D_0. \tag{5}$$

2.4. Compactibility. The compactibility was assessed by using the method used elsewhere by Mitrevej et al. [18] and also by Mužíková and Kubíčková [27]. The mean tablet breaking force values of 300 mg of the pregelatinized Taro Boloso-I starch according to the study design were tested 24 hr after compression at 12 kN. The compression force 12 kN was

Table 1: Experimental design for the pregelatinization study.

No.	Factor 1		Factor 2		Type of design point
	Coded X1	Actual Temperature (°C)	Coded X2	Actual Time (min)	
E1	-1.000	65.00	-1.000	20.00	Factorial design points
E2	+1.000	85.00	-1.000	20.00	
E3	-1.000	65.00	+1.000	60.00	
E4	+1.000	85.00	+1.000	60.00	
E5	-1.414	60.86	0.000	40.00	Axial design points
E6	+1.414	89.12	0.000	40.00	
E7	0.000	75.00	-1.414	11.72	
E8	0.000	75.00	+1.414	68.28	
E9-13	0.000	75.00	0.000	40.00	Central design points

selected for the optimization formulations because of two reasons. First, the densification of most of the compacts of the investigational starches including that of the starches modified at the central replica was observed to be plastic at or beyond 12 kN according to the Heckel plots besides it resulted in the strong compacts.

2.5. Optimization. Experimental designs: using circumscribed CCD, the effects of temperature and time of pregelatinization as factors on angle of repose, Hausner's ratio, Heckel's number, and TBF of the compacts prepared were evaluated. There were 13 experimental runs as shown in Table 1.

Polynomial regression algorithms were created using ANOVA output according to Design-Expert 8.0.7.1 (Stat-Ease, Corp. Australia) and used to predict the responses. Moreover, the factors were optimized by using numerical and graphical methods of optimization [23].

2.6. Validation and Comparison of Optimum Formulation. For validation of the models selected, tablet formulations at three points different from the design points were prepared, evaluated, and compared with the predicted values. For validation of the optimization result, the optimized product was prepared and compared as powder and in tablet formulations with the native starch.

2.7. Statistical Analyses. Statistical analyses including one-way ANOVA were applied by using Design-Expert 8.0.7.1 software (Stat-Ease, Corp. Australia) for the optimizations. The responses were expressed in polynomial models in terms of temperature and time of pregelatinization. All the results of the direct measurements were presented as arithmetic mean ± standard deviation. Origin version 7 (Origin LabTM Corporation, USA) was used to determine the lines of best fit. The target limit of the significance of statistical data was 95% CI.

3. Results and Discussion

3.1. Densities and Flow Properties. The density and flow properties of PGTBIS are presented in Table 2. The modifications increased bulk and tapped densities. However, it decreased true density most likely due to the hydrothermal disruption-related loosening of molecular packing and diffusion of amylose from the starch granules [28]. These effects were the highest at 89.12°C for 40 min as this temperature was higher than the endset temperature (84.40°C) [9] accompanied by complete disruption of the granular structure of the starch. The least decrease in true density was observed at 60.86°C for 40 min which shows that the temperature of gelatinization is associated directly with a decrease in its effect on the true density. The effects of true density reduction were lower also at 65°C for 20 min and 65°C for 60 min which are the temperature points below the onset temperature (68.40°C) where structural disruption of the starch granules is very insignificant. It gives the impression that the effect of gelatinization on the PGTBIS has some association with onset, peak, and endset temperatures of gelatinization which were 68.40°C, 75.46°C, and 84.40°C, respectively [9]. Generally, except for the points of pregelatinization at 60.86°C for 40 min and 65°C for 20 min, pregelatinization was shown to enhance flow property as it decreased the Carr index, Hausner ratio, and angle of repose and enabled the powder to flow. This was consistent with the published literature elsewhere [12].

3.2. Heckel's Plots. Compressibility leads to compactibility which per se leads to tabletability [29, 30]. The compressibility of pregelatinized starches was studied by Heckel's models. The results of Heckel's plots and parameters were as shown in Figure 1 and Table 3, respectively.

Figure 1 shows that all the Heckel plots start with nonlinear portions indicating that the initial densification is predominantly due to the rearrangement of particles. The next segment for all of the plots is linear suggesting a region where the dominant mechanism of densification is plastic deformation. The relevant parameters of the initial nonlinear and linear regions including spans of pressure are described in Table 3. The Heckel plot of the powder of the design point 85°C for 60 min was observed to have ups and downs. This is a sign of brittle fracture as a mechanism of deformation explained by secondary rearrangement phases of particles [18].

Table 2: Bulk, tapped, and true densities of the 13 pregelatinized starches.

T^* (°C)	T^{**} (min)	Density (gm/ml)			Hausner's ratio	Carr's index (%)	Angle of repose (°)	Flow rate (gm/s)
		Bulk	Tapped	True				
65.00	20.00	0.618 ± 0.00	0.746 ± 0.01	1.52 ± 0.05	1.20 ± 0.01	17.0 ± 0.7	30.8 ± 1.5	—
85.00	20.00	0.680 ± 0.00	0.797 ± 0.01	1.45 ± 0.03	1.17 ± 0.00	14.7 ± 0.2	18.9 ± 1.6	5.81 ± 0.10
65.00	60.00	0.683 ± 0.01	0.847 ± 0.00	1.50 ± 0.02	1.24 ± 0.01	19.3 ± 0.6	24.6 ± 1.4	2.50 ± 0.31
85.00	60.00	0.667 ± 0.01	0.828 ± 0.01	1.44 ± 0.04	1.22 ± 0.01	18.2 ± 1.0	15.6 ± 0.8	4.82 ± 0.92
60.86	40.00	0.506 ± 0.01	0.653 ± 0.02	1.55 ± 0.02	1.29 ± 0.01	22.5 ± 0.5	33.0 ± 0.5	—
89.12	40.00	0.663 ± 0.01	0.810 ± 0.01	1.43 ± 0.08	1.22 ± 0.01	18.1 ± 0.8	16.1 ± 3.5	6.06 ± 0.52
75.00	11.72	0.680 ± 0.03	0.776 ± 0.01	1.45 ± 0.01	1.14 ± 0.01	11.8 ± 0.7	21.2 ± 1.5	5.67 ± 0.84
75.00	68.28	0.701 ± 0.00	0.830 ± 0.01	1.45 ± 0.03	1.19 ± 0.01	15.8 ± 0.4	17.5 ± 1.6	5.48 ± 0.73
75.00	40.00	0.685 ± 0.01	0.833 ± 0.00	1.48 ± 0.08	1.22 ± 0.01	18.0 ± 0.6	20.7 ± 0.4	5.58 ± 0.69
75.00	40.00	0.705 ± 0.01	0.858 ± 0.01	1.47 ± 0.03	1.22 ± 0.00	18.1 ± 0.3	21.6 ± 0.8	5.65 ± 0.98
75.00	40.00	0.699 ± 0.02	0.838 ± 0.01	1.49 ± 0.03	1.20 ± 0.01	16.6 ± 0.7	20.9 ± 0.9	6.08 ± 0.75
75.00	40.00	0.660 ± 0.00	0.799 ± 0.00	1.46 ± 0.02	1.21 ± 0.00	17.4 ± 0.3	21.0 ± 0.4	6.06 ± 0.55
75.00	40.00	0.656 ± 0.00	0.787 ± 0.00	1.46 ± 0.07	1.20 ± 0.01	16.7 ± 0.5	21.8 ± 0.0	6.39 ± 0.71

T^* and T^{**} stand for temperature and time duration of pregelatinization.

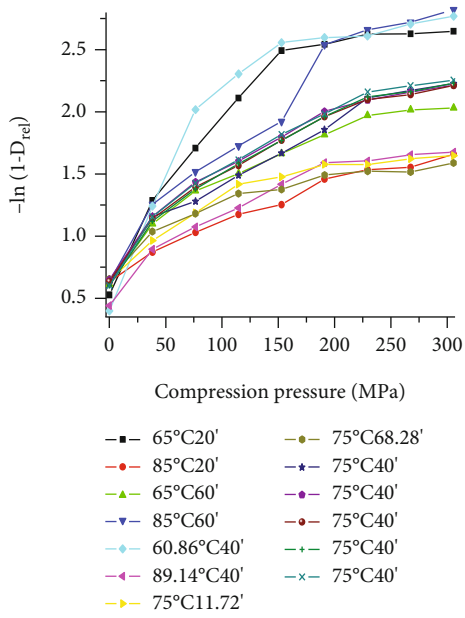

Figure 1: Heckel's plots of NTBIS pregelatinized at different conditions.

The results in Table 3 imply that the starch modified at 65°C for 20 min, 85°C for 20 min, 89.12 °C for 40 min, 75°C for 11.72 min, and 75°C for 68.28 min attained maximum densification before compression (relative density D_A) within 0-38.22 MPa span of compression pressure. At 38.22 MPa onwards, the particles of these powders start to deform and possibly form bonding. All the rest of the points including the 5 replicates at 75°C for 40 min start particulate deformation beyond this pressure observed at the point 76.43 MPa onwards. Likewise, plastic deformation of the powder extends highest (229.30 MPa) for the modification at 65°C for 60 min and 61°C for 20 min followed by all the 5 central replicate points and 89.12°C for 40 min (191.08 MPa). The maximum pressure for the plastic deformation was the least (114.65MPa) for the starches modified at 85°C for 20 min, 75°C for 12 min, and 75°C for 68 min. The largest region (152.87 MPa) of plastic deformation was observed at 65°C for 60 min. The Heckel yield pressure (P_y) was calculated from the inverse of the slope ($1/k$) of the linear portions. Accordingly, the modification at 65°C for 20 min had the smallest Heckel yield pressure ($P_y = 95.01$ MPa) followed by 141.66 MPa at 60.12°C for 40 min. The explanation might be that the temperature was too low to change the native nature of the starch granules which are small enough to be compressible [31, 32]. This indicates that the pregelatinization of the starch at 65°C for 20 min results in the most plastic deforming PGTBIS as evidenced by literature [21]. On the other hand, the least compressible powder ($P_y = 251.68$ MPa) was observed at 85°C for 20 min followed by 250.31 MPa observed at 65°C for 60 min and 249 MPa observed at 75°C for 68.28 min. Constant A is related to the particle rearrangement and die filling before deformation [22]. Constant "A" is related to particle rearrangement and die filling just before deformation and the bonding of discrete particles. It was used to calculate the total densification hitherto (D_A). According to the results, the powder at 60.86°C for 40 min showed the highest value for A (1.4844), the least being 0.7205 observed at 89.12°C for 40 min. The corresponding relative density (D_A) values were observed to be 0.7734 and 0.5135 indicating the powders to be the most and the least compressible, respectively. The phase of densification at low pressure (D_b) was calculated from the value of the D_A and the value of densification due to die filling (D_0). The powder at 60.86°C for 40 min showed the largest D_b (0.4368). Importantly, D_b exhibits a phase of densification at low

Table 3: Heckel's parameters of NTBIS pregelatinized at different conditions.

			Heckel's parameters						
T^* (°C)	T^{**} (min)	Range (MPa)	R^2	A_0	P_y	A	D_A	D_0	D_b
65.00	20.00	38.22-152.87	0.9998	0.5280	95.01	0.8948	0.5913	0.4114	0.1799
85.00	20.00	38.22-114.65	0.9997	0.6319	251.68	0.7219	0.5142	0.4466	0.0676
65.00	60.00	76.43-229.30	0.9998	0.6133	250.31	1.0530	0.6511	0.4584	0.1927
85.00	60.00	76.43-152.87	0.9999	0.6354	188.68	1.1143	0.6719	0.4663	0.2056
60.86	40.00	76.43-152.87	0.9992	0.3992	141.66	1.4844	0.7734	0.3366	0.4368
89.12	40.00	38.22-191.08	0.9996	0.4412	220.21	0.7205	0.5135	0.4440	0.0695
75.00	11.72	38.22-152.87	0.9999	0.6426	168.76	0.7374	0.5216	0.4788	0.0428
75.00	68.28	38.22-114.65	0.9994	0.6553	249.97	0.8812	0.5857	0.4498	0.1359
75.00	40.00	76.43-191.08	0.9995	0.6205	199.95	0.9044	0.5952	0.4639	0.1313
75.00	40.00	76.43-191.08	0.9990	0.6504	200.95	1.0435	0.6478	0.4781	0.1697
75.00	40.00	76.43-191.08	0.9996	0.6358	200.89	1.0081	0.6351	0.4746	0.1605
75.00	40.00	76.43-191.08	0.9998	0.6018	195.48	0.9956	0.6305	0.4496	0.1809
75.00	40.00	76.43-191.08	0.9992	0.6023	203.90	1.0544	0.6516	0.4496	0.2020

T^* and T^{**} stand for temperature and time duration of pregelatinization.

pressure and shows further densification due to particle fragmentation [18].

3.3. Compactibilities. The TBF and friability of compacts are described in Table 4.

The highest value of TBF was observed at 65°C for 20 min followed by the central replica indicating the compactibility. The modifications at 65°C for 20 min and 75°C for 12 min and all the 5 replicates at 75°C for 40 min had friability < 1.0% revealing appreciable cohesion of the compact particles [31, 33].

3.4. Analysis of Trends of Responses. Adequate mathematical models suitable for demonstrating the trends of responses graphically and mathematically were selected using the Design-Expert software. The values of angle of repose, Hausner's ratio, Heckel's yield pressure, and TBF values of the tablets were fed into the Design-Expert software. Then, for each of the responses, comparison of R^2, adjusted R^2, predicted R^2, and predicted residual sum of square (PRESS) values of linear, two-factor interaction (2FI), quadratic, and cubic models were undertaken. All the responses were found to best satisfy the quadratic polynomial model except for Heckel's yield pressure. The model of best fit for Heckel's yield pressure was shown to be the two-factor interaction model. These respective models which were suggested to satisfy the best had greater R^2 values (0.9846, 0.9470, 0.9394, 0.9585, and 0.9949), adjusted R^2 values (0.9736, 0.9091, 0.8961, 0.9447, and 0.9913) closer to 1 and in more reasonable agreement with the predicted R^2 values (0.9064, 0.7707, 0.7707, 0.8780, and 0.9778), and smaller predicted residual sum of square (PRESS) values (29.51, 0.0034, 0.0033, 3517.29, and 4.09) than any other nonaliased models [23]. The adequacy of these models for predicting the influences of the factors on the responses was verified by employing the ANOVA test. The model significance tests were such that $p < 0.0005$ and lack-of-fit tests were insignificant ($p > 0.05$) for all the five responses. Moreover, the adequate precision values, 36.86, 20.032, 12.564, 23.306, and 54.469 of the angle of repose, Hausner ratio, Heckel yield pressure, and TBF, respectively, showed that the signals are adequate and the respective models are quite valid. Two extra tests including the normal probability plots versus predicted values and the internally studentized residuals were also considered to prove the validity of the selected regression models. The normal probability plots of residuals versus predicted values reasonably approximated the normal plot of the predicted values. Similarly, the internally studentized residual values were <3 units away from zero and also randomly scattered for all the cases. These conditions further confirmed that the selected regression models were valid for the intended presentation of the trend of changes in responses in terms of the factors.

Table 4: TBF and friability of the compacts of the PGTBIS.

T^* (°C)	T^{**} (min)	TBF (N)	Friability
65	20	145.3 ± 7	0.2 ± 0.0
85	20	32.7 ± 4	Friable
65	60	48.3 ± 3	Friable
85	60	0.0 ± 0	Friable
60.86	40	17.0 ± 2	Friable
89.12	40	24.4 ± 2	Friable
75	11.72	59.4 ± 5	0.6 ± 0.0
75	68.28	0.0 ± 0	Friable
75	40	70.6 ± 5	0.6 ± 0.0
75	40	73.0 ± 5	0.5 ± 0.0
75	40	78.6 ± 6	0.4 ± 0.0
75	40	77.0 ± 7	0.6 ± 0.0
75	40	86.2 ± 6	0.5 ± 0.0

T^* and T^{**} stand for temperature and time duration of pregelatinization.

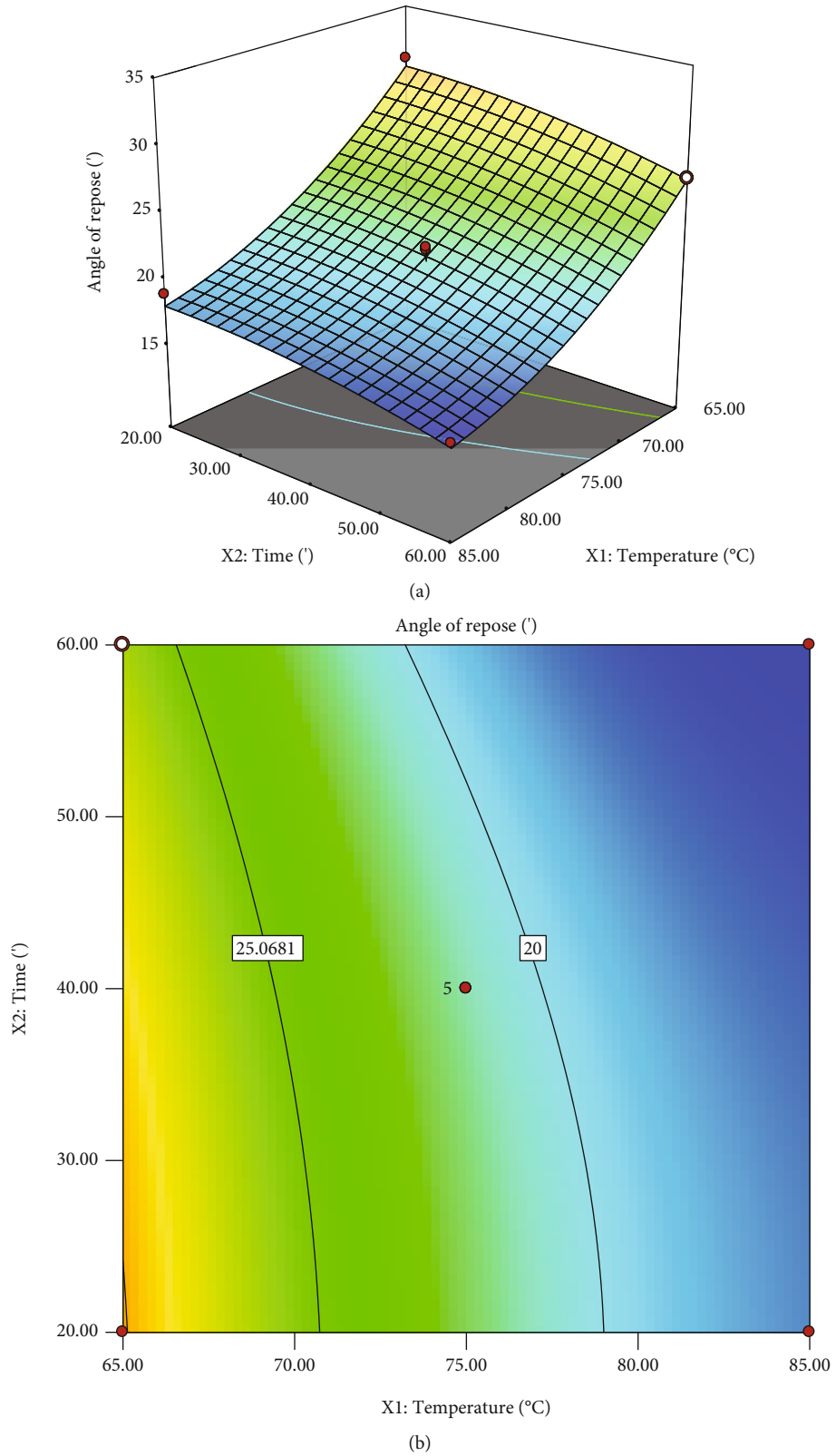

Figure 2: Surface response (a) and contour (b) plots of angle of repose versus the factors.

Having selected the models of best fits with statistically valid adequacy, equivalent mathematical equations were used to reveal the individual and interaction effects along with response surfaces. With this concern, equations (6) and (7) are the equations of angle of repose in terms of actual and coded factors, respectively, and used to predict the actual

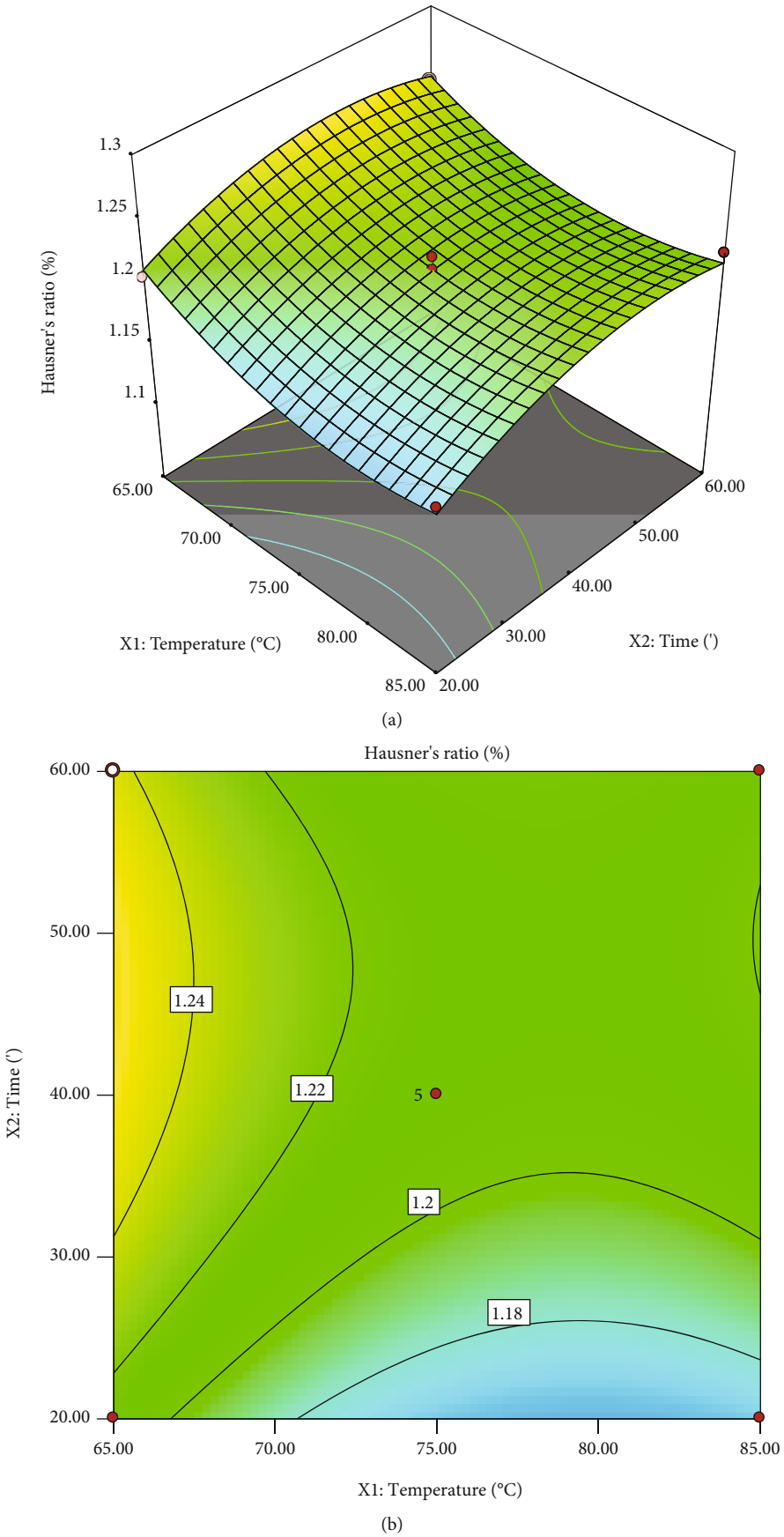

Figure 3: Surface response (a) and contour (b) plots of Hausner's ratio versus the factors.

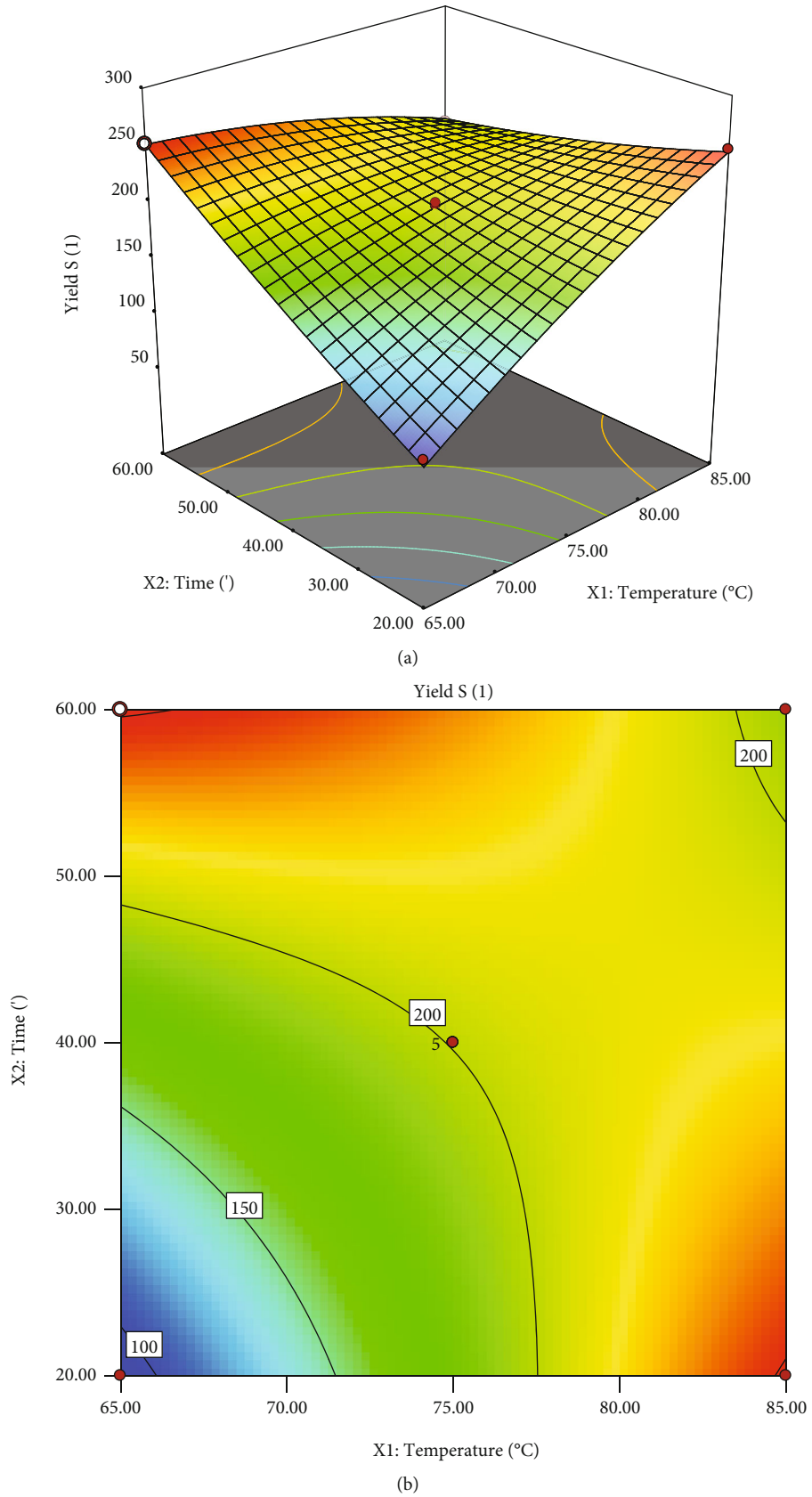

Figure 4: Surface response (a) and contour (b) plots of yield pressure versus the factors.

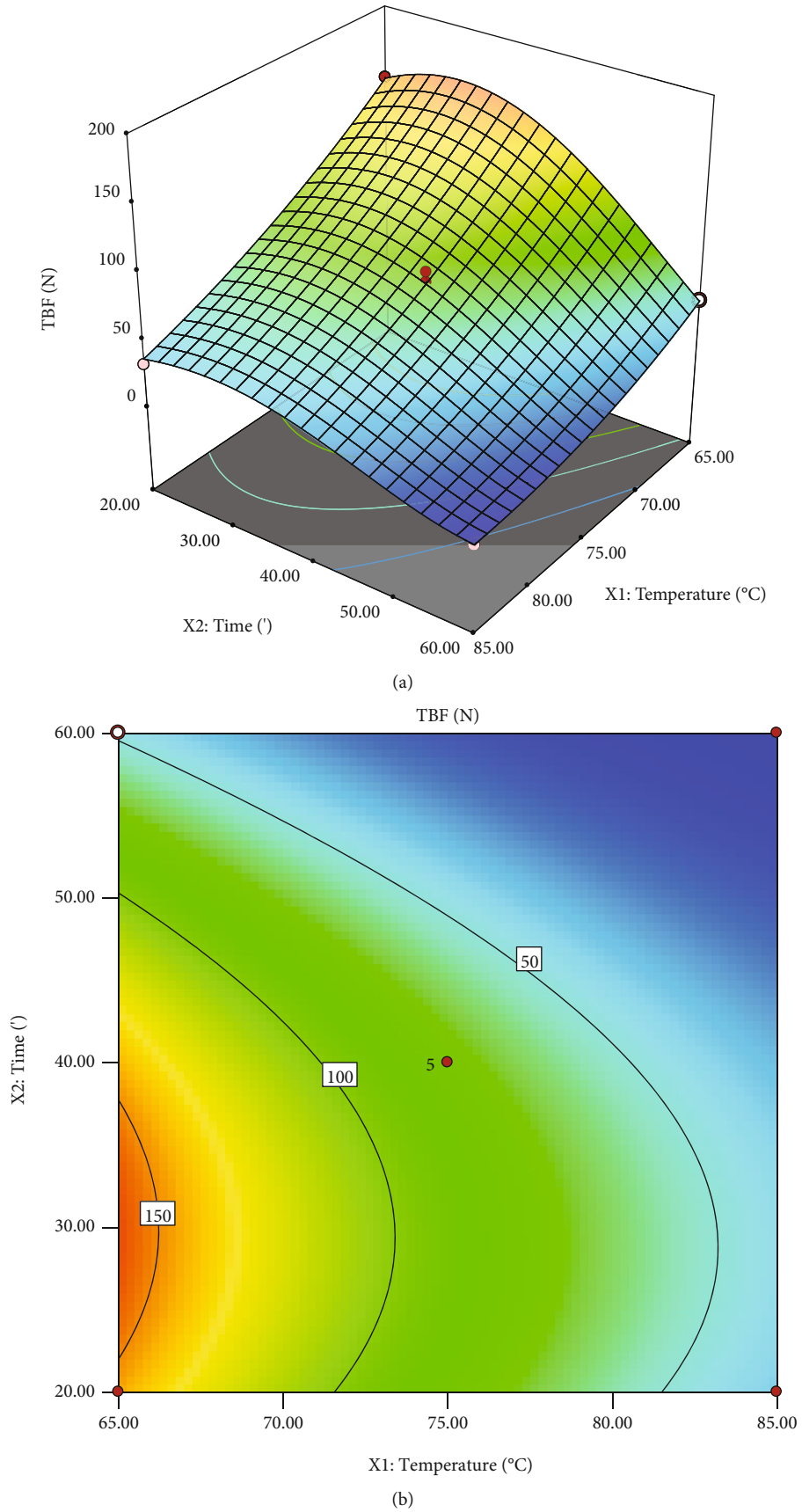

Figure 5: Surface response (a) and contour (b) plots of TBF versus the factors.

Table 5: Validation of the models selected.

Temperature (°C)		72	70	65
Time (min)		37	42	30
The angle of repose (°)	Experimental value	23.80 ± 0.5	24.05 ± 0.5	28.64 ± 0.8
	Predicted value	23.36	24.43	29.72
	Error	-1.88	1.56	3.63
Hausner's ratio	Experimental value	1.22 ± 0.02	1.24 ± 0.00	1.23 ± 0.01
	Predicted value	1.214	1.226	1.226
	Error	-0.824	-0.816	0.000
Heckel's yield pressure (MPa)	Experimental value	184.32	191.29	125.68
	Predicted value	185.27	190.23	126.06
	Error	0.51	-0.56	0.30
TBF (N)	Experimental value	102.32 ± 2.58	103.12 ± 1.08	153.43 ± 1.58
	Predicted value	101.41	101.53	159.69
	Error	-0.90	-1.57	3.92

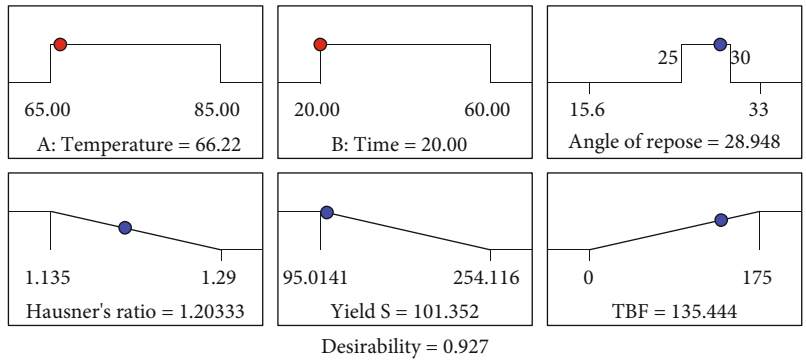

Figure 6: The ramps of optimum responses and factors from numerical optimization.

and relative impacts of each factor on angle of repose. Figure 2 shows the trend of angle of repose with changes in the temperature and time of pregelatinization diagrammatically.

$$\text{Angle of repose} = 177.591 - 3.526X_1 - 0.030X_2 + 0.019X_1^2, \quad (6)$$

where X_1 and X_2 are the actual values of temperature and time, respectively.

$$\text{Angle of repose} = 21.20 - 5.85X_1 - 1.59X_2 + 1.93X_1^2, \quad (7)$$

where X_1 and X_2 are the coded values of temperature and time, respectively.

Obviously, increase in both temperature and time decreases the angle of repose ($p < 0.0001$) and ($p = 0.0006$), respectively. This indicates enhancement of flow property supported by published report elsewhere about the effect of the modification by Adedokun and Itiola [24]. Temperature had positive quadratic effect on the angle of repose with coefficients of 1.93 ($p = 0.0003$).

For making prediction of the Hausner ratio for each of the levels of factors, the equation of the Hausner ratio in terms of actual values of factors is shown in equation (8). The same equation in terms of coded levels of the factors is given in equation (9). It is preferred for the estimation of the relative impact of each of the factors on the Hausner ratio. The trend of the Hausner ratio with changing levels of factors is diagrammatically depicted in Figure 3.

$$\text{Hausner's ratio} = 2.5785 - 0.0376X_1 + 0.0045X_2 + 0.000234X_1^2 - 0.00006X_2^2, \quad (8)$$

where X_1 and X_2 are the actual values of temperature and time, respectively.

$$\text{Hausner's ratio} = 1.21 - 0.0183X_1 + 0.0197X_2 + 0.0234X_1^2 - 0.0241X_2^2, \quad (9)$$

where X_1 and X_2 are the coded values of temperature and time, respectively.

The increase in temperature decreases the Hausner ratio as opposed to the time of pregelatinization. With coefficients of 0.0234 ($p = 0.0004$) and -0.0241 ($p = 0.0004$)

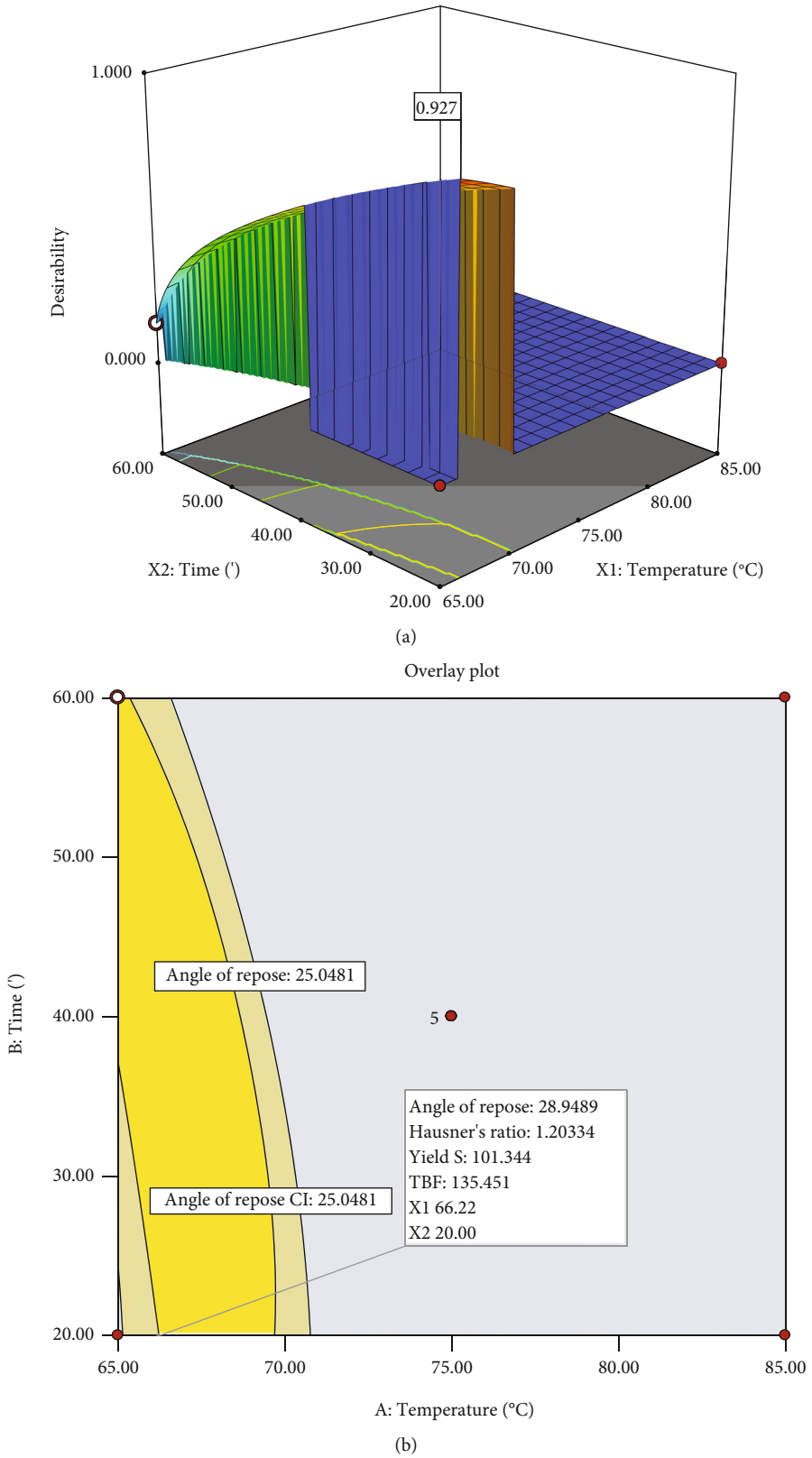

Figure 7: The overall desirability function RSM (a) and the overlay plot of responses (b).

of temperature and time of pregelatinization, respectively, positive and negative quadratic effects on the Hausner ratio were observed.

The prediction of Heckel's yield pressure could be made by using its equation in terms of the actual values of each of the factors (equation (10)). The relative impacts of each of

the variables on the Heckel yield pressure could also be determined by equation (11) in which it is expressed in terms of coded levels of each of the variables. The 3D graphical demonstration of changes in the Heckel yield pressure with changing levels of the factors is presented in Figure 4.

$$P_y = -1378.65 + 27.61X_1 + 21.03X_2 - 0.28X_1X_2 - 0.09X_1^2 + 0.01X_2^2, \quad (10)$$

where P_y, X_1, and X_2 are the actual values of Heckel's yield pressure, temperature, and time, respectively.

$$P_y = 200.60 + 25.94X_1 + 25.87X_2 - 55.44X_1X_2 - 9.29X_1^2 + 5.27X_2^2, \quad (11)$$

where P_y, X_1, and X_2 are the coded values of Heckel's yield pressure, temperature, and time, respectively.

The Heckel yield pressure was observed to increase with increasing levels of both temperature (coefficient of 25.94, $p < 0.0001$) and time (coefficient of 25.87, $p < 0.0001$). The interaction of the two factors antagonized the Heckel yield pressure with a factor of 55.44 ($p < 0.0001$).

In the same fashion, the compactibility property with changing levels of actual values of the factors in the design space was predictable using equation (12). The relative impacts of each of the factors on the TBF were evident from its equation in terms of the coded levels of factors (equation (13)). The trend TBF with changing levels of the factors is diagrammatically presented in 3D (Figure 5).

$$\sqrt{\text{TBF}} = 29.86 + 0.406X_1 + 0.428X_2 - 0.00633X_2^2, \quad (12)$$

where TBF, X_1, and X_2 stand for tablet breaking force and actual values of temperature and time, respectively.

$$\sqrt{\text{TBF}} = 8.77 - 3.13X_1 - 2.71X_2 - 2.53X_2^2, \quad (13)$$

where TBF, X_1, and X_2 stand for tablet breaking force and coded values of temperature and time, respectively.

Both temperature and time of pregelatinization exhibited negative effect on the square root of TBF with coefficients of -3.13 ($p < 0.0001$) and -2.71 ($p < 0.0001$), respectively. The time of pregelatinization was observed to have a negative quadratic effect on the square root of TBF with a coefficient of -2.53 ($p < 0.0001$).

Finally, the models selected were validated by pregelatinization of the same starch at three points other than the design points and comparing experimentally determined levels of responses with the predicted values (Table 5).

None of the responses in the selected data points showed as high as ±5% error with respect to the predicted value verifying that the models selected could demonstrate the trend of responses with changing levels of the factors within the design space.

3.5. Optimization. To optimize the factors towards the goals of the responses, the numerical (Figures 6 and 7(a)) and graphical (Figure 7(b)) methods of optimization were used [23].

The region of design space protruding upwards in Figure 7(a) and shaded with yellow color in Figure 7(b) represents the set of points fulfilling the criteria limited in the constraints. In these diagrams, the desirability flag and selected point show the point suggested as optimum with respect to all the responses considered. As a result, the optimum condition of pregelatinization was 66.22°C for 20 min resulting in the angle of repose of 28.95°, HR of 1.20, Heckel yield pressure of 101.35 MPa, and TBF of the tablet of 135.45 N with the desirability of 0.910 indicating that this point is the most desirable with respect to the goals of each of the responses.

Table 6: Densities and flow properties of NTBIS and PGTBIS.

	PGTBIS	NTBIS*	Starch 1500®
D [3, 4] (μm)	176.65	2.36	—
Bulk density (g/ml)	0.62 ± 0.00	0.45 ± 0.00	0.61 ± 0.01
Tapped density (g/ml)	0.74 ± 0.00	0.56 ± 0.00	0.73 ± 0.01
True density (g/ml)	1.53 ± 0.01	1.56 ± 0.01	1.49 ± 0.02
Carr's index (%)	16.85 ± 0.43	23.1 ± 0.70	16.61 ± 0.18
Hausner's ratio	1.20 ± 0.01	1.30 ± 0.01	1.20 ± 0.00
Angle of repose (°)	29.53 ± 0.1	—	26.59 ± 0.4
Flow rate (g/s)	5.83 ± 0.7	—	5.5 ± 0.6

*Report adopted from our previous publication [9].

3.6. Validation of the Optimization and Comparative Evaluation of Optimized Starch. In order to validate the optimization result, the optimized pregelatinized Taro Boloso-I starch (PGTBIS) was prepared by heating 15% slurry of the NTBIS at 66.22°C for 20 minutes. Then, the angle of repose, Hausner ratio, Heckel Yield pressure, and tablet breaking strength of the PGTBIS and the Starch 1500® were determined. The PGTBIS was compared with the NTBIS and Starch 1500® in terms of the bulk density, tapped density, true density, Hausner ratio, and Carr index which are presented in Table 6.

The particle size, D [3, 4], of PGTBIS determined using laser light diffractometer (176.65 μm) was by far higher than that of NTBIS reported in our previous publication (2.36 ± 0.05 μm) [9, 34]. Both bulk density (0.62 ± 0.00 g/ml) and tapped density (0.74 ± 0.00 g/ml) of PGTBIS were higher than NTBIS ($p < 0.05$) may be due to changes in particle sizes and shapes [35]. Density values are related to total, interparticle, and intraparticle porosities which in turn indicate the properties of excipients like compressibility and tablet disintegrating potential and are also related to flow properties [31]. The higher bulk density is advantageous for it reduces fill volume during tableting. The angle of repose value of PGTBIS (29.53 ± 0.1°) was higher than that of the Starch 1500® (26.59 ± 0.4°) ($p < 0.05$) indicating that it might have lower flowability. However, both the PGTBIS and Starch 1500® were within the range of excellent flowability index (25-30°) in USP/NF [36]. The Carr index of PGTBIS

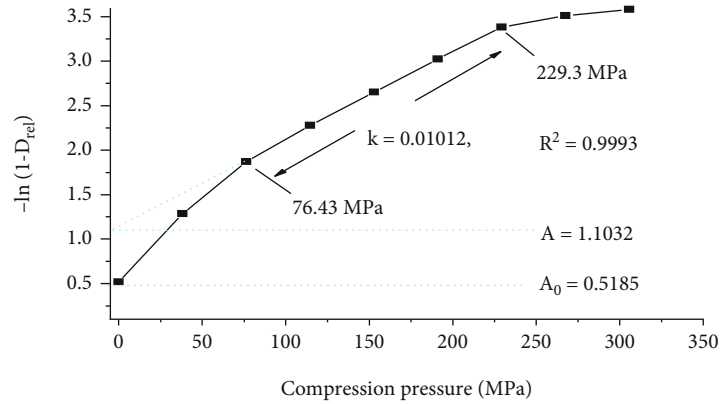

Figure 8: Heckel's plot of PGTBIS.

Table 7: The properties of tablets PGTBIS compressed at 12 kN.

Starch type	Hardness (N)	Friability (%)
PGTBIS	134.8 ± 5.3	0.27 ± 0.01
NTBIS	138.0 ± 7.5	0.25 ± 0.02
Starch 1500®	86.1 ± 0.44	0.52 ± 0.01

(16.85 ± 0.43%) was comparable to that of the Starch 1500® (16.61 ± 0.18%) ($p > 0.05$) but noticeably lower than that of NTBIS (23.1 ± 0.70%) ($p < 0.05$). These values of Carr's index gave a good promise regarding the compressibility and hence the tabletability of the powder [36]. The reason for low Carr's index could be low interparticular interaction which favors compressibility. It was in the range of values claimed to be fair in flow according to the USP/NF classification of the flowability [37]. The reason for enhancement of the flow property of PGTBIS compared to that of the NTBIS might be due to increment of the particle size more than 100-folds as the experimental findings clearly show. This is consistent with literature [38]. Observation of the true density values determined for use in Heckel's parameters has shown that the pregelatinization slightly decreased the true density from 1.56 ± 0.02 g/ml to 1.53 ± 0.01 g/ml ($p < 0.05$). This could possibly be owing to hydrothermal disruption of crystal structure and diffusion of amylose molecules out of the granules [28]. Accordingly, PGTBIS has statistically comparable density to that of Starch 1500® (1.49 ± 0.02) ($p > 0.05$). The Heckel plot of the PGTBIS was constructed and is shown in Figure 8. The shape of the Heckel plot and parameters from its linear segment (slope, k, and intercept, A) were used for the exploration of mechanisms of deformation, the extent of plastic deformation, and the influence of rearrangement or fragmentation during pressure-induced densification of powders. Initial densification of PGTBIS gives the impression that it is due to rearrangement or fragmentation of the powder particles revealed by the nonlinearity. The linear segment ($R^2 = 0.9997$) of the plot suggests that the granules deform plastically in the range compression pressure 76.43-229.30 MPa. The Heckel yield pressure (P_y) was calculated from the inverse of the slope ($k = 0.01012\ \text{MPa}^{-1}$) and equals 98.81 MPa with error of only 2.6% from the predicted value 101.45 MPa. The Heckel yield pressure reported in this study was lower than the Heckel yield pressure values of MCC, mannitol, lactose, and dicalcium phosphate reported elsewhere [39]. The implication is the PGTBIS powder could have better plasticity and compressibility. Moreover, the Heckel constant "A" (1.1039) shows the total densification of the powder bed before deformation and corresponds to $D_A = 0.6786$. The phase of densification by rearrangement before the particles of powder start individual deformation and possible bonding was found to be $D_b = 0.2743$.

For the insight of compactibility profiles, TBF and friability of tablets compressed at 12 kN of pure PGTBIS, NTBIS, and the Starch 1500® were investigated (Table 7). The TBF of the pure PGTBIS tablet was 134.8 ± 5.3 N which shows that the mean value was almost similar to the predicted value (135.4 N). The TBF value of the native starch compressed at the same pressure was 138.0 ± 7.5 N which shows that the decrease in the compactibility of the Taro Boloso-I starch following pregelatinization was not statistically significant ($p > 0.05$). The tablets of Starch 1500® compressed at the same compression pressure had lower TBF value (86.1 ± 0.44) than that of PGTBIS ($p < 0.05$). Besides, the friability of tablets of PGTBIS was lower than that of the Starch 1500® ($p < 0.05$) and statistically comparable to the friability of compacts of the NTBIS ($p > 0.05$). The TBF and friability data observed in this study suggest that PGTBIS would have better compactibility than the Starch 1500®. The confirmation results verify that the analysis and optimization processes were well represented and valid in the mathematical models and the optimization. Since the pregelatinized starch has ensured to have good flowability and compactibility, it can be considered as a promising direct compression excipient for pharmaceutical tablet dosage forms. In comparison to the Starch 1500® as a filler and binder in direct compression tablets, the PGTBIS has comparable flow properties but better compactibility. The better compactibility might be because of formation of interparticular bridges to better extent with all other necessary preconditions such as presence of optimum moisture [40]. The PGTBIS could therefore be considered in the direct compression tablet formulations instead of the Starch 1500®.

4. Conclusions and Recommendations

An increase in both temperature and time of pregelatinization of Taro Boloso-I starch enhanced its flowability. The Heckel yield pressure was observed to increase with the increase in levels of both temperature and time. Both temperature and time of pregelatinization were found to have decreasing effects on compressibility/compactibility. Pregelatinization had a trade-off effect on compressibility and flowability. Heating at 66.22°C for 20 min was the optimum point of pregelatinization for balanced and acceptable flowability and compressibility/compactibility. At this point, sufficient flowability and compressibility/compactibility were achieved indicated by the angle of repose of $29.56 \pm 0.24^{\circ}$, Hausner ratio of 1.20 ± 0.01, Heckel yield pressure of 104.4 MPa, and TBF of 138.0 N at a compression force of 12 kN. Accordingly, it was discovered that the PGTBIS starch could be taken as a potential direct compression excipient. Its novelty is that the PGTBIS could perform better as filler and binder in direct compression tablets than the Starch 1500® in terms of compactibility. Further investigations including brittle fracture index, Young's modulus, toughness, lubricant sensitivity, and dilution potential studies by using specific drugs should be performed towards its application in pharmaceutical industries.

Data Availability

The authors confirm that all the data associated with this paper are available upon request.

Conflicts of Interest

The authors declare no conflict of interest.

Acknowledgments

The authors would like to thank Areka Town Administration and School of Pharmacy, Addis Ababa University, for this is part of the work presented to its institutional repository as a thesis [41] (although there are significant improvements). The authors also appreciate Areka Agricultural Research Center for the material donations and Ethiopian Pharmaceutical Manufacturing Share Company (EPHARM) for the access to laboratory facilities. The abstract of this article has also been shortlisted as the one to be presented in proceedings of the 2nd Global Conference on Pharmaceuticals and Clinical Research to be held in 2023, Dubai, UAE [42].

References

[1] Q. T. Zhou and T. Li, "Formulation and manufacturing of solid dosage forms," *Pharmaceutical Research*, vol. 36, no. 1, pp. 1–3, 2018.

[2] N. Al-Zoubi, S. Gharaibeh, A. Aljaberi, and I. Nikolakakis, "Spray drying for direct compression of pharmaceuticals," *PRO*, vol. 9, no. 2, p. 267, 2021.

[3] H. Murakami, T. Yoneyama, K. Nakajima, and M. Kobayashi, "Correlation between loose density and compactibility of granules prepared by various granulation methods," *International Journal of Pharmaceutics*, vol. 216, no. 1-2, pp. 159–164, 2001.

[4] D. Natoli, M. Levin, L. Tsygan, and L. Liu, "Development, optimization, and scale-up of process parameters: tablet compression," in *Developing solid oral dosage forms, Pharmaceutical theory and practice*, Y. Qiu, Y. Chen, G. G. Zhang, L. Liu, and W. R. Porter, Eds., pp. 725–759, Elsevier, Inc., New York, 2009.

[5] M. Z. Ahmad, S. Akhter, M. Anwar, M. Rahman, M. A. Widdiquib, and F. J. Ahmad, "Compactibility and compressibility studies of Assam Bora rice starch," *Powder Technology*, vol. 224, pp. 281–286, 2012.

[6] I. D. Pedro, I. C. Brandão, G. M. Souza, and G. Carneiro, "Development of tablet formulations of calcium carbonate by direct compression," *Journal of Applied Pharmaceutical Science*, vol. 4, pp. 12–20, 2017, https://www.academia.edu/35060434/Development_of_tablet_formulations_of_calcium_carbonate_by_direct_compression.

[7] R. Benabbas, N. M. Sanchez-Ballester, A. Aubert, T. Sharkawi, B. Bataille, and I. Soulairol, "Performance evaluation of a novel biosourced co-processed excipient in direct compression and drug release," *Polymers*, vol. 13, no. 6, p. 988, 2021.

[8] T. B. Balla, M. J. Nisha, and A. Belete, "In vitro evaluation of native Taro Boloso-I starch as a disintegrant in tablet formulations," *Advances in Materials Science and Engineering*, vol. 2021, Article ID 7576730, 10 pages, 2021.

[9] T. B. Balla, M. J. Nisha, and A. Belete, "Isolation and physicochemical characterization of starch from Taro Boloso-I tubers," *Indian Drugs*, vol. 55, no. 7, pp. 20–27, 2018.

[10] Y. Hong, G. Liu, and Z. Gu, "Recent advances of starch-based excipients used in extended-release tablets: a review," *Drug Delivery*, vol. 23, no. 1, pp. 12–20, 2016.

[11] M. V. Tupa, L. Altuna, M. L. Herrera, and M. L. Foresti, "Preparation and characterization of modified starches obtained in acetic anhydride/tartaric acid medium," *Starch–Stärke*, vol. 72, no. 5-6, article 1900300, 2020.

[12] O. A. Odeku, W. Schmid, and K. M. Picker-Freye, "Material and tablet properties of pregelatinized (thermally modified) Dioscorea starches," *European Journal of Pharmaceutics and Biopharmaceutics*, vol. 70, no. 1, pp. 357–371, 2008.

[13] M. A. Garcia, C. F. Garcia, and A. A. Faraco, "Pharmaceutical and biomedical applications of native and modified starch: a review," *Starch–Stärke*, vol. 72, no. 7-8, article 1900270, 2020.

[14] B. Chaudhuri, A. Mehrotra, F. J. Muzzio, and M. S. Tomassone, "Cohesive effects in powder mixing in a tumbling blender," *Powder Technology*, vol. 165, no. 2, pp. 105–114, 2006.

[15] M. V. Lawal, "Modified starches as direct compression Excipients - Effect of physical and chemical modifications on tablet properties: a review," *Starch–Stärke*, vol. 71, no. 1-2, article 1800040, 2019.

[16] M. V. Lawal, M. A. Odeniyi, and O. A. Itiola, "Material and rheological properties of native, acetylated, and pregelatinized forms of corn, cassava, and sweet potato starches," *Starch–Stärke*, vol. 67, no. 11-12, pp. 964–975, 2015.

[17] R. W. Heckel, "Density-pressure relationship in powder compaction," *Transaction of the Metallurgical Society of AIME*, vol. 221, pp. 671–675, 1961.

[18] A. Mitrevej, D. Faroongsarng, and N. Sinchaipanid, "Compression behavior of spray dried rice starch," *International Journal of Pharmaceutics*, vol. 140, no. 1, pp. 61–68, 1996.

[19] C. M. Gabaude, M. Guillot, J. C. Gautier, P. Saudemon, and D. Chulia, "Effects of true density, compacted mass, compression speed, and punch deformation on the mean yield pressure," *Journal of Pharmaceutical Sciences*, vol. 88, no. 7, pp. 725–730, 1999.

[20] C. Bache, P. M. Olsen, P. Bertelsen, and J. M. Sonnergaard, "Compressibility and compactibility of granules produced by wet and dry granulation," *International Journal of Pharmaceutics*, vol. 358, no. 1-2, pp. 69–74, 2008.

[21] G. Vreeman and C. C. Sun, "Mean yield pressure from the in-die Heckel analysis is a reliable plasticity parameter," *International Journal of Pharmaceutics*, vol. 3, article 100094, 2021.

[22] R. T. Widodo and A. Hassan, "Compression and mechanical properties of directly compressible pregelatinized sago starches," *Powder Technology*, vol. 269, pp. 15–21, 2015.

[23] G. A. Lewis, D. Mathieu, and R. Phan-Tan-luu, *Pharmaceutical Experimental Design*, Marcel Dekker, Inc., New York, USA, 1998, https://www.routledge.com/Pharmaceutical-Experimental-Design/Lewis-Mathieu-Phan-Tan-Luu/p/book/9780367447748.

[24] M. O. Adedokun and O. A. Itiola, "Disintegrant activities of natural and pregelatinized trifoliate yams, rice and corn starches in paracetamol tablets," *Journal of Applied Pharmaceutical Science*, vol. 1, pp. 200–206, 2011, https://www.japsonline.com/admin/php/uploads/328_pdf.pdf.

[25] M. H. Othman, G. M. Zayed, U. F. Ali, and A. A. H. Abdellatif, "Colon-specific tablets containing 5-fluorouracil microsponges for colon cancer targeting," *Drug Development and Industrial Pharmacy*, vol. 46, no. 12, pp. 2081–2088, 2020.

[26] H. M. Tawfeek, M. Roberts, M. A. El Hamd, A. A. H. Abdellatif, and M. A. Younis, "Glibenclamide mini-tablets with an enhanced pharmacokinetic and pharmacodynamic performance," *AAPS PharmSciTech*, vol. 19, no. 7, pp. 2948–2960, 2018.

[27] J. Mužíková and A. Kubíčková, "A study of compressibility and compactibility of directly compressible tableting materials containing tramadol hydrochloride," *Acta Pharmaceutica*, vol. 66, no. 3, pp. 433–441, 2016.

[28] H. D. Belitz, W. Grosch, and P. Schieberle, *Food Chemistry*, Springer, Berlin, 4th edition, 2009, https://www.academia.edu/23725260/Food_Chemistry_4th_Edition_by_Belitz_W_Grosch_P_Schieberle_1.

[29] M. Santl, I. Ilic, F. Vrecer, and S. Baumgartner, "A compressibility and compactibility study of real tableting mixtures: the impact of wet and dry granulation versus a direct tableting mixture," *International Journal of Pharmaceutics*, vol. 414, no. 1-2, pp. 131–139, 2011.

[30] A. ElShaer, P. Hanson, and A. R. Mohammed, "A systematic and mechanistic evaluation of aspartic acid as filler for directly compressed tablets containing trimethoprim and trimethoprim aspartate," *European Journal of Pharmaceutics and Biopharmaceutics*, vol. 83, no. 3, pp. 468–476, 2013.

[31] J. Swarbrick, *Encyclopedia of Pharmaceutical Technology*, Informa Healthcare, New York, USA, 3rd edition, 2007, https://gmpua.com/Process/EncyclopediaPT.pdf.

[32] S. Abdel-Hamid, F. Alshihabi, and G. Betz, "Investigating the effect of particle size and shape on high speed tableting through radial die-wall pressure monitoring," *International Journal of Pharmaceutics*, vol. 413, no. 1-2, pp. 29–35, 2011.

[33] T. Y. Puttewar, M. D. Kshirsagar, A. V. Chandewar, and R. V. Chikhale, "Formulation and evaluation of orodispersible tablet of taste masked doxylamine succinate using ion exchange resin," *Journal of King Saud University-Science*, vol. 22, no. 4, pp. 229–240, 2010.

[34] C. Siriwachirachai and T. Pongjanyakul, "Particle agglomeration of acid-modified tapioca starches: characterization and use as direct compression fillers in tablets," *Pharmaceutics*, vol. 14, no. 6, p. 1245, 2022.

[35] B. Johansson and G. Alderborn, "The effect of shape and porosity on the compression behaviour and tablet forming ability of granular materials formed from microcrystalline cellulose," *European Journal of Pharmaceutics and Biopharmaceutics*, vol. 52, no. 3, pp. 347–357, 2001.

[36] Y. Akdag, T. Gulsun, N. Izat, M. Cetin, L. Oner, and S. Sahin, "Characterization and comparison of deferasirox fast disintegrating tablets prepared by direct compression and lyophilization methods," *Journal of Drug Delivery Science and Technology*, vol. 57, article 101760, 2020.

[37] USP-NF, *1174 Powder Flow*, The United States Pharmacopeial Convention, Rockville, MD, USA, 2011.

[38] G. Ren, C. Clancy, T. M. Tamer, B. Schaller, G. M. Walker, and M. N. Collins, "Cinnamyl O-amine functionalized chitosan as a new excipient in direct compressed tablets with improved drug delivery," *International Journal of Biological Macromolecules*, vol. 141, pp. 936–946, 2019.

[39] J. Zhang, C. Wu, X. Pan, and C. Wu, "On identification of critical material attributes for compression behaviour of pharmaceutical diluent powders," *Materials*, vol. 10, no. 7, p. 845, 2017.

[40] R. T. Widodo, A. Hassan, K. B. Liew, and L. C. Ming, "A directly compressible pregelatinised sago starch: a new excipient in the pharmaceutical tablet formulations," *Polymers*, vol. 14, no. 15, p. 3050, 2022.

[41] T. B. Balla, M. J. Nisha, and A. Belete, *Evaluation of taro Boloso-I native (Colocasia esculenta cultivar) starch as disintegrant and its pre-gelatinized form as direct compression diluent in paracetamol tablets, [M.S. thesis]*, Addis Abeba University, 2016.

[42] T. B. Balla, M. J. Nisha, and A. Belete, "Optimization of pregelatinized Taro Boloso-I starch as a directly compressible excipient," in *In Proceedings of the 2nd Global Conference on Pharmaceuticals and Clinical Research*, Dubai, UAE, 2023https://www.pharmaceutical.scientexconference.com/speakers/Tamrat-Balcha-Balla.